ACADEMIC PRESS

Available online at www.sciencedirect.com

SCIENCE DIRECT®

Journal of Sound and Vibration 260 (2003) 287–305

JOURNAL OF SOUND AND VIBRATION

www.elsevier.com/locate/jsvi

A non-linear fluid force model for vortex-induced vibration of an elastic cylinder

X.Q. Wang*, R.M.C. So, K.T. Chan

Department of Mechanical Engineering, The Hong Kong Polytechnic University, Hung Hom, Kowloon, Hong Kong

Received 5 March 2001; accepted 29 April 2002

Abstract

Even under the assumption of a sinusoidal lift and drag force at a single frequency for a stationary cylinder in a cross flow, higher harmonics that represent non-linearity in the fluid–structure interaction process are present. This fact is considered in the formulation of a non-linear fluid force model for a freely vibrating cylinder in a cross flow. The force model is developed based on an iterative process and the modal analysis approach. The fluid force components in the model can be evaluated from measured vibration data with the help of the auto-regressive moving averaging (ARMA) technique. An example is used to illustrate that non-linear (higher order) force components are present at resonance, even for a case with relatively weak fluid–structure interaction. Further analysis reveals that the fluid force components are dependent on structural damping and mass ratio. The non-linear fluid force model is further modified by taking these considerations into account and is used to predict the dynamic characteristics of a freely vibrating cylinder over a range of Reynolds numbers, mass and structural damping ratios. On comparison with measurements obtained from four different experiments and predictions made by previous single-degree-of-freedom model, good agreement is found over a wide range of these parameters.

1. Introduction

Vortex-induced vibration of a circular cylinder is one of the fundamental problems in flow-induced vibration. For a cylinder in a cross flow, the flow separates and vortex streets are formed in the wake of the cylinder when the Reynolds number based on D and U_∞ exceeds a critical value. The vortices are alternately shed from the cylinder. This vortex shedding induces an approximately periodic excitation on the cylinder and causes it to vibrate. The structural vibration

*Corresponding author.
E-mail address: mmxqwang@polyu.edu.hk (X.Q. Wang).

0022-460X/03/$ - see front matter
PII: S0022-460X(02)00945-8

modifies the flow, which in turn alters the induced force acting on the cylinder. The resulting fluid–structure interaction is a non-linear process and will give rise to structural vibration with multiple frequencies [1,2].

Much effort has been made to investigate the underlying mechanism of the fluid-structure interaction resulting from vortex-induced cylinder vibration. The investigations include experimental, numerical, empirical and theoretical studies. Empirical modelling of flow-induced vibration has been reviewed in books [1,2] and articles [3–5]. In general, the empirical models can be classified into two groups: one is the force decomposition model, and the other is the wake-oscillator model. Sarpkaya [6] introduced the concept of force decomposition and used it to analyze vortex-induced vibration of an elastically supported rigid cylinder. The fluid force was decomposed into two components, a fluid inertia force and a fluid damping force related to the cylinder displacement and velocity, respectively. Griffin and Koopmann [7] and Griffin [8] divided the fluid force into an excitation part and a reaction part; the latter included all motion-dependent force components. On the other hand, Chen et al. [9] proposed an unsteady flow theory to model vortex-induced vibration. The fluid force was assumed to be dependent on the displacement, velocity, and acceleration of the cylinder. This force was expressed as a linear combination of the motion-dependent components. The component in-phase with the cylinder displacement was treated as a fluid stiffness force, while the fluid inertia force was calculated from potential flow theory. In all these models, data collected from free and forced vibration experiments was used to determine the fluid force components and they were shown to be dependent on U_r and Y, the vibration amplitude. When the model was used to predict X and Y, Sarpkaya [6] suggested an iteration technique, thus allowing the fluid–structure interaction effects to be accounted for, at least partially.

In a wake-oscillator model, a Van de Pol-type equation was invoked as the governing equation of the lift force. This equation was coupled to the cylinder dynamic equation through one or several terms related to the cylinder dynamics. Hartlen and Currie [10] were the first to propose the wake-oscillator model. Their proposal was motivated by the suggestion of Bishop and Hassan [11]. There was some mathematical basis for the Van de Pol equation. Based on a fluid dynamic analysis, Iwan and Blevins [12] obtained a model similar to that proposed by Hartlen and Currie [10]. The Van de Pol model was later modified by a number of researchers [13–17] in order to obtain better agreement with experimental measurements and to replicate experimental observations, such as the hysteresis phenomenon, the cellular vortex pattern in a shear flow, etc.

In these empirical models, only Y was considered, and a single-degree-of-freedom (s.d.o.f.) dynamics model was used to analyse the structural motion. In practice, however, X and Y are coupled in any flow-induced vibration problem. Therefore, in order to obtain a better understanding of flow-induced vibration, at least a two-degree-of-freedom (2.d.o.f.) dynamics model should be invoked, along with a fluid force model that takes into account the fluid forces in both the x and y directions. Furthermore, for a finite cylinder, the displacement varies along the span, thus making the modelling of the fluid force more complicated. Skop and Griffin [18] and Iwan [19] extended the wake-oscillator model to the case of a single elastic cylinder. Other researchers [20, 21] used the concept of spanwise correlation to model this flow-induced vibration problem. Beyond that, there are few studies carried out to account for the effects of spanwise variation of X and Y.

The present paper focuses on an empirical study, whereby a non-linear fluid force model is sought to replicate the actual flow-induced forces experienced by a finite structure in a free vibration case. The model attempts to account for the effects of X and Y and their variations along the cylinder span. Even under the assumption of sinusoidal fluid forces at a single frequency for a stationary cylinder, fluid–structure interaction introduces higher harmonics to the fluid forces. The appearance of the higher harmonics could be accounted for by invoking the modal analysis method and using it together with the auto-regressive moving averaging (ARMA) technique to indirectly evaluate from measured cylinder displacements the fluid force components in the model.

The ARMA technique was originally developed as a time-domain modal analysis method. In this technique, a general multi-degree-of-freedom (m.d.o.f.) system is considered. The equation of motion for this system is represented by an ARMA model, in which the current value of the system response is expressed as a linear combination of past values of the excitation and the response, plus a white noise. The coefficients in the model are determined so that it provides a best fit to the measured time series in the sense of maximum likelihood. Once the coefficients are determined, natural frequencies, damping ratios, and mode shapes can be obtained from the auto-regressive part of the ARMA model. A more detailed description of this technique is given in Ref. [22].

The force components thus deduced are used to predict vortex-induced vibration of a freely vibrating long slender cylinder and the associated fluid–structure interaction. The structural damping and mass ratio, ζ_s and M_r, could further influence the dynamic motions of the cylinder. Taking ζ_s and M_r into account in the evaluation of the force components further modifies the model. Thus formulated, it can be used to analyze flow-induced vibration problems over a wide range of Re, ζ_s, M_r, and U_r. Therefore, the cumbersome numerical solutions of the full set of Navier–Stokes equations and its coupling to the structural dynamics equations could be avoided. Finally, predictions obtained from this model are compared with experimental data and predictions by s.d.o.f. model in the literature.

2. A fluid force model

2.1. Formulation

The free vibration of an elastically supported rigid circular cylinder in a uniform cross flow is considered. The flow is assumed to be two dimensional when the cylinder aspect ratio is sufficiently large. In most considerations, the cylinder is assumed to be infinitely long, therefore, a spring–damper–mass system can be used to model the cylinder vibration in a cross-section of the cylinder as illustrated in Fig. 1. For a cylinder with a large aspect ratio, this assumption is only applicable in an approximate sense. The co-ordinate system is chosen so that x represents the streamwise direction, y the transverse direction, and z the axis of the cylinder, which is vertical to the page and not shown in the figure. The origin of the co-ordinate system is located at the center of the cylinder.

In a force decomposition model, the fluid force is usually expressed as a sinusoidal function of time at the vortex shedding frequency. This might be valid for a stationary cylinder as suggested

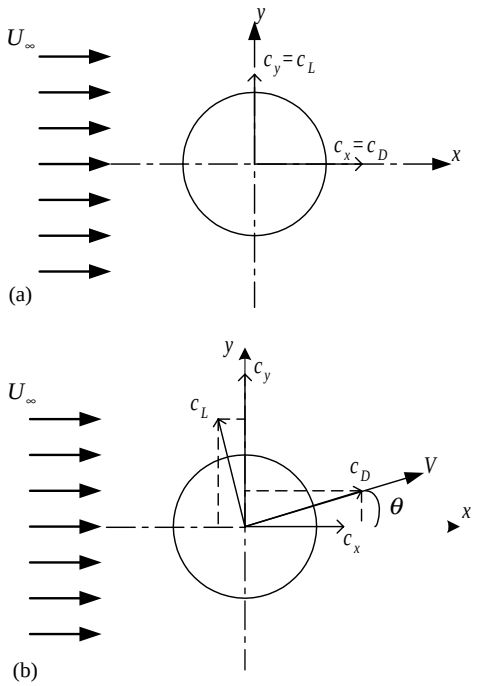

Fig. 1. Illustration of one cross-section of a cylinder in a cross flow and the fluid forces exerted on it: (a) stationary cylinder, (b) vibrating cylinder.

by Bishop and Hassan [11] and supported by the analysis of Olinger and Sreenivasan [23]. They showed that there is only one dominant frequency and that is the vortex shedding frequency. For an oscillating cylinder, the spectrum of the wake velocity shows that sub- and super-harmonics are also present. Experimental study of the free vibration of a single and two side-by-side elastic cylinders in a cross flow [24,25] also showed that the frequency spectrum of the vibration displacement includes the response peaks at higher harmonics of the shedding frequency. This is evidence of the presence of non-linearity in the fluid–structure interaction.

For a stationary cylinder, the lift and drag force coincides with the x- and y-axis, respectively, as shown in Fig. 1a. However, when the cylinder is vibrating as a result of vortex shedding, the lift (F_L) and drag (F_D) forces do not coincide with the x- and y-axis, respectively, due to the relative motion of the cylinder, as shown in Fig. 1b. The corresponding force coefficients exerted on the cylinder can thus be expressed as

$$c_x(t) = c_D(t)\cos\theta - c_L(t)\sin\theta, \tag{1a}$$

$$c_y(t) = c_D(t)\sin\theta + c_L(t)\cos\theta. \tag{1b}$$

The meaning of these symbols and those following are defined in Appendix A. It should be pointed out that all force coefficients are defined with respect to ρ, U_∞, D and unit span of the cylinder. Throughout this paper, all quantities and equations, unless otherwise specified, are made

dimensionless with respect to U_∞ and D. In Eqs. (1a) and (1b), θ is the angle between the x-axis and the instantaneous velocity vector of the cylinder motion and is given by

$$\theta(t) = \text{arctg}\left(\frac{\dot{Y}(t)}{U_\infty - \dot{X}(t)}\right) = \text{arctg}\left(\frac{\dot{Y}(t)}{1 - \dot{X}(t)}\right), \tag{2}$$

where the dot denotes differentiation with respect to time, t. Since, in general, $\dot{X}$ and $\dot{Y}$ are smaller than 1, the angle θ is very small and

$$\sin\theta(t) = \frac{\dot{Y}(t)}{\sqrt{\dot{Y}^2(t) + (1 - \dot{X}(t))^2}} \approx \dot{Y}(t), \tag{3a}$$

$$\cos\theta(t) = \frac{1 - \dot{X}(t)}{\sqrt{\dot{Y}^2(t) + (1 - \dot{X}(t))^2}} \approx 1. \tag{3b}$$

Eq. (1) can thus be simplified to

$$c_x(t) = c_D(t) - c_L(t)\,\dot{Y}(t), \tag{4a}$$

$$c_y(t) = c_D(t)\,\dot{Y}(t) + c_L(t). \tag{4b}$$

For an elastically supported rigid cylinder, a 2.d.o.f. model is assumed, therefore, the equations of motion are given by

$$\ddot{X}(t) + 2\zeta_s\omega_{n0}\dot{X}(t) + \omega_{n0}^2 X(t) = \frac{c_x(t)}{2M_r}, \tag{5a}$$

$$\ddot{Y}(t) + 2\zeta_s\omega_{n0}\dot{Y}(t) + \omega_{n0}^2 Y(t) = \frac{c_y(t)}{2M_r}. \tag{5b}$$

Together, Eqs. (4) and (5) constitute the governing equations of the system. These equations actually represent an iteration process as shown below.

The iteration process starts from the situation in which the cylinder is stationary. For a stationary cylinder, F_L and F_D are assumed to be sinusoidal at the vortex shedding frequency f_s and at $2f_s$, respectively, thus, they can be written as

$$c_D(t) = \bar{C}_D + C_D\sin(2\omega_s t + \phi_D), \tag{6a}$$

$$c_L(t) = C_L\sin(\omega_s t + \phi_L). \tag{6b}$$

where ϕ_D and ϕ_L are phase angles by which F_D and F_L lead the transverse displacement of the cylinder. Since $\dot{Y}(t) = 0$ for a stationary cylinder, $c_x = c_D$ and $c_y = c_L$. Therefore,

$$c_x(t) = \bar{C}_{D0} + C_D\sin(2\omega_s t + \phi_D), \tag{7a}$$

$$c_y(t) = C_{L0}\sin(\omega_s t + \phi_L). \tag{7b}$$

Using Eq. (5), the cylinder response is calculated to be $Y(t) = Y_{max}\sin\omega_s t$ and $X(t) = \bar{X} + X_{max}\sin(2\omega_s t + \phi_X)$, where ϕ_X is the phase angle by which X leads Y. The cylinder vibrations will alter the fluid forces, and the effects are two-fold. Firstly, the cylinder vibrations change the

geometry of the flow field in the fluid–structure boundary, thus altering the magnitudes of C_L and C_D. Secondly, the cylinder vibrations change the angle θ and alter f_x and f_y, as can be seen by substituting the expression for $Y(t)$ into Eq. (4) and obtaining

$$c_x(t) = C_x^{(0)} + C_{x,m}^{(2)} \sin 2\omega_s t + C_{x,d}^{(2)} \cos 2\omega_s t, \tag{8a}$$

$$c_y(t) = C_{y,m}^{(1)} \sin \omega_s t + C_{y,d}^{(1)} \cos \omega_s t + C_{y,m}^{(3)} \sin 3\omega_s t + C_{y,d}^{(3)} \cos 3\omega_s t. \tag{8b}$$

Detailed derivation of Eq. (8) is given in Appendix B. The fluid force coefficients, $C_x^{(0)}$, $C_{x,m}^{(2)}$, $C_{x,d}^{(2)}$, $C_{y,m}^{(1)}$, $C_{y,d}^{(1)}$, $C_{y,d}^{(3)}$, and $C_{y,m}^{(3)}$, represent various fluid force components. For example, the subscript d stands for fluid damping force which is related to the velocity of the cylinder, and m denotes a combination of fluid stiffness and fluid inertia (added mass) forces which are related to the displacement and the acceleration of the cylinder, respectively. In Appendix B are given the expressions of these force coefficients, and it can be seen that they are functions of the displacement amplitude, the vortex shedding frequency, and such system parameters as the natural frequency of the combined fluid–cylinder system and the structural damping.

Compared with the fluid forces for a stationary cylinder, it can be seen that the free vibration of an elastic cylinder introduces a 3rd harmonic to the transverse fluid force. As a result, the response of the cylinder includes this 3rd harmonics accordingly. It can be expected that, when this iteration process goes on as shown in Fig. 2, other higher harmonics would gradually appear in the fluid forces, and the cylinder responses at these higher harmonics are in turn excited. The order of the higher harmonics in the fluid forces and the cylinder vibrations is thus increased during the iteration process. In this sense, the present model can be regarded as a marching process in the frequency domain for the study of vortex-induced vibration problems.

When the cylinder vibrations are stable, the cylinder vibrations and the fluid forces would asymptotically converge to

$$c_x(t) = C_x^{(0)} + \sum_{k=1}^{\infty} C_{x,m}^{(2k)} \sin[(2k)\omega_s t] + C_{x,d}^{(2k)} \cos[(2k)\omega_s t], \tag{9a}$$

$$c_y(t) = \sum_{k=1}^{\infty} C_{y,m}^{(2k-1)} \sin[(2k-1)\omega_s t] + C_{y,d}^{(2k-1)} \cos[(2k-1)\omega_s t], \tag{9b}$$

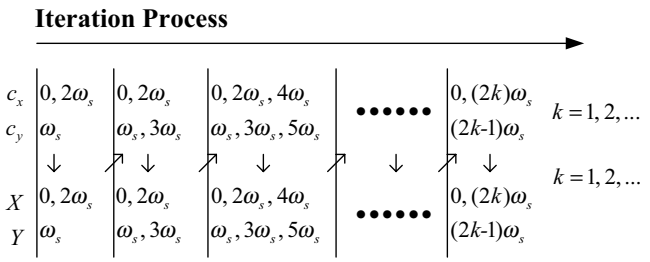

Fig. 2. Illustration of the iteration process in which higher harmonics are gradually introduced into the fluid forces and cylinder vibrations due to fluid–structure interaction.

and

$$X(t) = \bar{X} + \sum_{k=1}^{\infty} X_{max}^{(2k)} \sin[(2k)\omega_s t], \tag{10a}$$

$$Y(t) = \sum_{k=1}^{\infty} Y_{max}^{(2k-1)} \sin[(2k-1)\omega_s t]. \tag{10b}$$

If only basic (first) harmonic components of the fluid force in Eq. (9b) are considered, the resulting fluid force representation is in the same form as that given in Ref. [6], who used the concept of force decomposition to deduce the force components. Mathematically, the present representation can thus be regarded as an extension of Sarpkaya's model to include the effects of higher harmonics. However, the interpretation is not that simple. It should be pointed out that the addition of higher harmonics has their physical meaning, because the appearance of the higher harmonics arises from the coupling of the fluid flow equations with the structural dynamic equations, or they represent the important fluid–structure interaction effect.

2.2. Extension to a finite cylinder with fix-support

Next, a more general case of a finite elastic cylinder in a cross flow is considered. The cylinder is assumed to be a slender one fix-supported at both ends. However, its vibration is modelled by the Euler–Bernoulli beam theory because of the finiteness of the cylinder length. The equation of motion in dimensional form is expressed as

$$m\frac{\partial^2 X(z,t)}{\partial t^2} + c\frac{\partial X(z,t)}{\partial t} + EI\frac{\partial^4 X(z,t)}{\partial z^4} = F_x(z,t), \tag{11a}$$

$$m\frac{\partial^2 Y(z,t)}{\partial t^2} + c\frac{\partial Y(z,t)}{\partial t} + EI\frac{\partial^4 Y(z,t)}{\partial z^4} = F_y(z,t). \tag{11b}$$

Using the modal analysis approach, the equation of motion (in dimensionless form) can be written as

$$\ddot{X}_n(z,t) + 2\zeta_{sn}\omega_{n0}\dot{X}_n(z,t) + \omega_{n0}^2 X_n(z,t) = \frac{f_{xn}(z,t)}{2M_r}, \quad n = 1,2,\ldots, \tag{12a}$$

$$\ddot{Y}_n(z,t) + 2\zeta_{sn}\omega_{n0}\dot{Y}_n(z,t) + \omega_{n0}^2 Y_n(z,t) = \frac{f_{yn}(z,t)}{2M_r}, \quad n = 1,2,\ldots, \tag{12b}$$

where

$$f_{xn}(z,t) = W_n(z)\int_{-L/2}^{L/2} c_x(z,t)W_n(z)\,\mathrm{d}z, \quad n = 1,2,\ldots, \tag{13a}$$

$$f_{yn}(z,t) = W_n(z)\int_{-L/2}^{L/2} c_y(z,t)W_n(z)\,\mathrm{d}z, \quad n = 1,2,\ldots. \tag{13b}$$

The displacement and velocity of the vibrating cylinder are given by

$$X(z,t)=\sum_{n=1}^{\infty}X_n(z,t),\qquad \dot{X}(z,t)=\sum_{n=1}^{\infty}\dot{X}_n(z,t), \tag{14a}$$

$$Y(z,t)=\sum_{n=1}^{\infty}Y_n(z,t),\qquad \dot{Y}(z,t)=\sum_{n=1}^{\infty}\dot{Y}_n(z,t). \tag{14b}$$

An elastically supported rigid cylinder can be regarded as a special case of the present formulation where only the rigid-body mode exists. The rigid-body mode can be represented by the mode of $n=0$ for which $W_n(z)=1$ and the fluid force is uniform along the cylinder span. However, for the present more general case, the fluid forces may not be uniform along the span. Their variations could be represented by

$$c_x(z,t)=\sum_{p=1}^{\infty}c_{xp}(t)W_p(z), \tag{15a}$$

$$c_y(z,t)=\sum_{p=1}^{\infty}c_{yp}(t)W_p(z). \tag{15b}$$

The modal force can then be expressed as

$$f_{xn}(z,t)=c_{xn}(t)W_n(z)\int_{-L/2}^{L/2}W_n^2(z)\,\mathrm{d}z=c_{xn}(t)W_n(z),\quad n=1,2,\ldots, \tag{16a}$$

$$f_{yn}(z,t)=c_{yn}(t)W_n(z)\int_{-L/2}^{L/2}W_n^2(z)\,\mathrm{d}z=c_{yn}(t)W_n(z),\quad n=1,2,\ldots, \tag{16b}$$

where $\int_{-L/2}^{L/2}W_n^2(z)\,\mathrm{d}z=1$ for a normal mode.

This is equivalent to carrying out a modal analysis of the fluid forces, and it can be seen that the modal fluid force for each mode, $c_{xn}(t)$ and $c_{yn}(t)$, $n=1,2,\ldots$, is assumed to be independent of z. Therefore, Eqs. (9a) and (9b) can be used to approximate them for the case of an elastically supported rigid cylinder.

3. Evaluation of fluid force components

The fluid force components in the proposed model can be evaluated by spectral analysis of the time histories of the fluid forces. Since the fluid forces are difficult to measure in general, an alternative way is to derive them indirectly from the measured data of cylinder vibration. Granger [26] has developed a modal identification method for this purpose. In his method, the fluid force is modelled as the addition of a force induced by flow turbulence and a force due to fluid-elastic phenomenon, the latter including all motion-dependent forces. In the present paper, the fluid force model is developed based on an iterative process simulating the fluid–structure interaction, and the formulae for evaluating fluid force components are derived below.

3.1. Evaluation formula

In order to determine the fluid force components from the measured cylinder displacements, a relation between the fluid forces and the corresponding cylinder vibrations needs to be established. Consider the cylinder vibration in the transverse direction first. Substituting Eq. (9b) into Eq. (16b) gives

$$f_{yn}(z,t) = W_n(z)\left\{\sum_{k=1}^{\infty} C_{yn,m}^{(2k-1)} \sin[(2k-1)\omega_s t] + C_{yn,d}^{(2k-1)} \cos[(2k-1)\omega_s t]\right\}, \quad n = 1, 2, \ldots. \tag{17}$$

The equation of motion can now be written as

$$\ddot{Y}_n(z,t) + 2\zeta_{sn}\omega_{n0}\dot{Y}_n(z,t) + \omega_{n0}^2 Y_n(z,t) = \frac{W_n(z)}{2M^*}\left\{\sum_{k=1}^{\infty} C_{yn,m}^{(2k-1)} \sin[(2k-1)\omega_s t] + C_{yn,d}^{(2k-1)} \cos[(2k-1)\omega_s t]\right\}, \quad n = 1, 2, \ldots. \tag{18}$$

Noting that the cylinder response can be expressed similarly to Eq. (10b) as

$$Y_n(z,t) = \sum_{k=1}^{\infty} Y_{n,max}^{(2k-1)}(z)\sin[(2k-1)\omega_s t], \tag{19}$$

the force coefficients in Eq. (18) can be derived from Eq. (12b). The results are

$$C_{yn,m}^{(2k-1)} = \frac{2M_r}{W_n(z)}\{\omega_{n0}^2 - [(2k-1)\omega_s]^2\}\, Y_{n,max}^{(2k-1)}(z), \quad k, n = 1, 2, \ldots, \tag{20a}$$

$$C_{yn,d}^{(2k-1)} = \frac{2M_r}{W_n(z)}(2\zeta_{sn}\omega_{n0})(2k-1)\omega_s\, Y_{n,max}^{(2k-1)}(z), \quad k, n = 1, 2, \ldots. \tag{20b}$$

Similarly, using Eq. (12a) for the streamwise vibration, the corresponding force coefficients are

$$C_{xn,m}^{(2k)} = \frac{2M_r}{W_n(z)}\{\omega_{n0}^2 - [(2k)\omega_s]^2\}\, X_{n,max}^{(2k)}(z), \quad k, n = 1, 2, \ldots, \tag{21a}$$

$$C_{xn,d}^{(2k)} = \frac{2M_r}{W_n(z)}(2\zeta_{sn}\omega_{n0})(2k)\omega_s X_{n,max}^{(2k)}(z), \quad k, n = 1, 2, \ldots. \tag{21b}$$

In the above derivation, the static deformation of the cylinder due to the mean drag is neglected since only the fluctuating part is of interest here.

In order to evaluate all the force components, the frequency of vortex shedding and the maximum displacements of the cylinder at the shedding frequency and its harmonics for each mode have to be known. This is carried out in two steps. Firstly, the measured cylinder vibration is decomposed as

$$Y(z,t) = \sum_{n=1}^{\infty} Y_n(t) W_n(z), \tag{22}$$

where $Y_n(t)$ is a series of time functions representing individual contribution of each normal mode to the total displacement. Secondly, the power density spectrum of each modal displacement, $Y_n(t)$, is calculated using the ARMA technique. From the calculated frequency spectrum, the

angular frequency of vortex shedding, ω_s, and the individual contributions of the cylinder displacement at the shedding frequency and its higher order harmonics, $Y_{n,max}^{(2k-1)}(z)$, $k = 1, 2, \ldots$, are determined. Then, the fluid force components are deduced from Eq. (20). For the x direction, the same procedure also applies.

It should be pointed out that this way of evaluating the force components neglects the effects of ζ_s and M_r. At this point, it is not clear how large these effects would be. Therefore, it is prudent to first examine the validity of the model before making further improvements to the force components. This will be carried out in Section 4 after the model has been validated against several cases where experimental measurements are available, and an approach is proposed to further improve the force components if the validation is not quite satisfactory.

3.2. An example

An example is given below to demonstrate the procedure of evaluating the fluid force components from the measured data of cylinder vibration. The example is taken from the experiment of So et al. [24], where the transverse vibration of a fixed–fixed elastic circular cylinder in a cross flow was measured over a range of *Re*. The parameters of the fluid–structure system used in the experiment are given in Table 1, and the readers are referred to Ref. [24] for details of the experimental setup and measurement procedure.

Two cases in the experiment are considered in the present example; one is a resonance case with $U_{r1} = 4.5$, another is an off-resonance case with $U_{r1} = 16.4$. Resonance is defined as the situation where the vortex shedding frequency is approximately equal to the fundamental natural frequency of the cylinder. In the off-resonance case, the shedding frequency is between the second and the third natural frequencies.

The analysis of the fluid force components presented above covers the whole frequency range, from zero to infinity. In a practical case, however, only a finite frequency range needs to be considered, that is, $k = 1, 2, \ldots, K$, and $n = 1, 2, \ldots, N$ in Eqs. (20a) and (20b). The limits, K and N, are determined from the analysis of the frequency spectrum of the cylinder vibration. For the two experimental cases, the frequency spectra of the cylinder displacement, calculated using ARMA, are plotted in Fig. 3. In the resonance case, there is only one dominant frequency. This was identified to be the vortex shedding frequency as well as the fundamental natural frequency of the cylinder. Several small frequency peaks were also discernable. These can be interpreted to represent the higher harmonics of the shedding frequency and the third natural frequency of the cylinder. The lowest frequency peak has been identified to be caused by low-frequency noise and, therefore, should be disregarded. In the off-resonance case, the vortex shedding frequency does not coincide with any one of the natural frequencies of the cylinder, thus four frequency peaks are

Table 1
Structural parameters of the cylinder

Material	L (mm)	D (mm)	M_r	Natural frequencies (Hz) and damping ratios (in stationary air)			
Acrylic	350.0	6.0	455.0	$f_{n1}^* = 99$ $\zeta_{s1} = 0.03$	$f_{n2}^* = 272$ $\zeta_{s2} = 0.02$	$f_{n3}^* = 534$ $\zeta_{s3} = 0.017$	$f_{n4}^* = 883$ $\zeta_{s4} = 0.01$

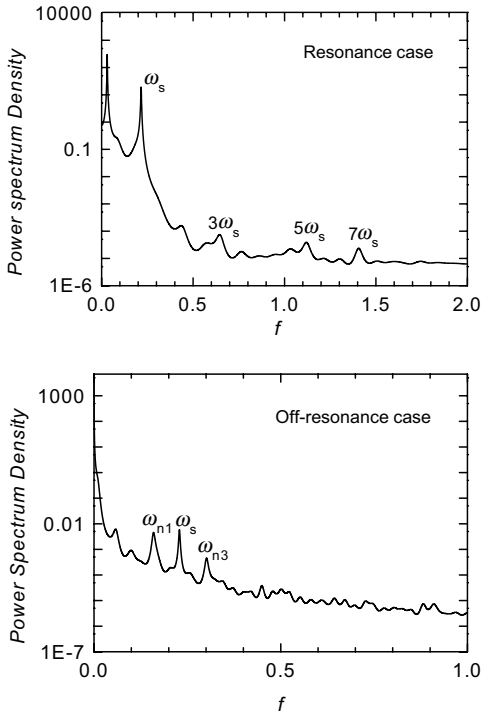

Fig. 3. Power spectral density (PSD) of the mid-span displacement of an elastic cylinder in a cross flow.

observed and are almost equally dominant. These peaks represent the vortex shedding frequency and the first three natural frequencies of the cylinder, respectively. The higher harmonics of the shedding frequency are rather small. This is expected since higher harmonics are the result of fluid–structure interaction, which is weak in this off-resonance case.

From the above analysis of the frequency spectra of the two experimental cases, it can be determined that only the responses of the first four normal modes need to be considered in the present example, that is, $N = 4$. The highest order of the higher harmonics is taken to be 7, that is, $K = 4$ for the resonance case, while $K = 1$ for the off-resonance case. The fluid force components for these two cases are then evaluated. Firstly, the components of cylinder displacement, $Y_{n,max}^{(2k-1)}(z)$, $k = 1, 2, \ldots, K$, and $n = 1, 2, \ldots, N$, are determined. The vortex shedding frequency is determined from the ARMA analysis and the force components are evaluated using Eqs. (20a) and (20b). The results are listed in Tables 2 and 3.

3.3. Discussion

The total fluid force in the y direction is given by

$$f_y(z,t) = \sum_{n=1}^{N} W_n(z) \left\{ \sum_{k=1}^{K} C_{yn,m}^{(2k-1)} \sin[(2k-1)\omega_s t] + C_{yn,d}^{(2k-1)} \cos[(2k-1)\omega_s t] \right\}, \tag{23}$$

Table 2
Fluid force components for the resonance case

	$n=1$	$n=3$		$n=1$	$n=3$
$C_{yn,m}^{(1)}$	0.0126	0.0529	$C_{yn,d}^{(1)}$	0.0138	2.5433×10^{-3}
$C_{yn,m}^{(3)}$	2.4895×10^{-5}	1.0496×10^{-4}	$C_{yn,d}^{(3)}$	8.1424×10^{-5}	1.5054×10^{-5}
$C_{yn,m}^{(5)}$	1.3632×10^{-5}	5.7466×10^{-5}	$C_{yn,d}^{(5)}$	7.1419×10^{-5}	1.3202×10^{-5}
$C_{yn,m}^{(7)}$	1.3954×10^{-6}	5.8824×10^{-5}	$C_{yn,d}^{(7)}$	9.9430×10^{-5}	1.8378×10^{-5}

Table 3
Fluid force components for the off-resonance case

	$n=1$	$n=3$		$n=1$	$n=3$
$C_{yn,m}^{(1)}$	−0.4266	0.2420	$C_{yn,d}^{(1)}$	8.1598×10^{-3}	8.7854×10^{-3}

which is assumed to be sinusoidal at the vortex shedding frequency when the cylinder is stationary. When the cylinder is excited by the fluid flow, the motion of the cylinder modifies the fluid force. The effects of cylinder motion on the fluid forces are two-fold in general. Firstly, cylinder motion might alter the lift and drag forces, their frequencies and amplitudes by changing the pressure distribution around the cylinder. Secondly, cylinder motion might introduce higher order harmonics to the fluid force. In the present model, F_L and F_D are always assumed to be sinusoidal at a single frequency regardless of whether the cylinder is stationary or vibratory. Under this assumption, all higher order components can be considered as due to the fluid–structure interaction, as can be seen from the development of the model.

An analysis of the fluid force components is instructive for the understanding of fluid–structure interaction. An example is given in which the fluid force at the mid-span of the cylinder ($z=0$) is analyzed. Considering the resonance case, the fluid force is expressed as

$$\begin{aligned} f_y(0,t) = &-0.0870\sin\omega_s t + 0.0311\cos\omega_s t \\ &- 1.7284\times10^{-4}\sin3\omega_s t + 1.8314\times10^{-4}\cos3\omega_s t \\ &- 0.9463\times10^{-4}\sin5\omega_s t + 1.6064\times10^{-4}\cos5\omega_s t \\ &- 1.3041\times10^{-4}\sin7\omega_s t + 2.2365\times10^{-4}\cos7\omega_s t. \end{aligned} \tag{24}$$

For the off-resonance case, the fluid force is expressed as

$$f_y(0,t) = 1.6912\sin\omega_s t + 1.7607\times10^{-3}\cos\omega_s t. \tag{25}$$

It can be seen that a linear expression of the fluid force is adequate for the off-resonance case and suggests that fluid–structure interaction at off-resonance only increases the magnitude of the originally linear fluid force but would not give rise to any significant higher order harmonics. At resonance, however, non-linear fluid force components of odd orders are obvious, although the amplitudes of these non-linear components are much smaller than that of the linear counterparts. This can be attributed to the fact that both the mass ratio (M_r =455) and the structural damping

(ζ_{s1} =0.03, ζ_{s2} =0.02, and ζ_{s3} =0.017) in the experimental study are large, thus the resulting cylinder displacement is small, leading to a relatively weak fluid–structure interaction. Nevertheless, the non-linear components are clearly observed.

4. Prediction of vortex-induced vibration

The model is then used to predict vortex-induced vibration of a cylinder in three experiments, where the measurements have been previously reported [7,27–29]. In Table 4 are listed the parameters of the fluid–structure systems tested in these three experiments.

The measured peak values of the maximum displacement of the cylinder for these cases are listed in Table 4, along with the predictions, designated here as Prediction 1, for comparison. These peak values occur at around $U_r = 5$, thus the fluid force components obtained from the resonance case ($U_{r1} = 4.5$) of So et al. [24] is used in the prediction. In all three cases considered, the predictions are smaller than the measured data. This could be attributed to the large difference in structural parameters specified in the experiment of So et al. [24] and the three other experiments [7,27–29]. The So et al. [24] experiment has high ζ_s and M_r, while the other three experiments have drastically lower values (Table 4). The values used in Ref. [24] are at least two orders of magnitude larger than those given in the other three experiments. It is obvious that the effects of M_r and ζ_s cannot be accounted for properly if the fluid force components obtained from one case is directly used to predict vibration amplitude in another case where the structural properties are completely different.

Table 4
Comparison of present predictions with experimental results

	Griffin and Koopmann [7]		Brika and Laneville [27]	Khalak and Williamson [28,29]	So et al. [24]
	System I	System II			
Re	738	760	7350	6000	994
f_n	0.1633	0.1587	0.1768	0.1883	0.2150
M_r	36.82	131.93	660	2.4	455
ζ_s	0.00068	0.00033	0.00008 + 0.00010Y2	0.0054	0.03
$\delta_r = 2\pi\zeta_s M_r$	0.1571	0.2733	0.3318	0.0817	85.7655
$C_{y1,m}^{(1)}$	0	0	NA	NA	−0.0870
$C_{y1,d}^{(1)}$	0.0501	0.0476	NA	NA	0.0311
Comparison of Y_{max}					
Measured	0.475	0.275	0.4	0.94	0.00034
Prediction 1	0.1495	0.0888	0.0679	0.2064	0.00034
Prediction 2	0.4752	0.2749	0.1468	1.0680	0.00031
Prediction 3	0.4752	0.2749	0.1482	0.7128	0.00031
Sarpkaya's prediction [6]	0.43	0.24	—	—	—

In fact, the force components, whose expressions after the first iteration are given in Appendix B, are shown to be dependent on the system parameters. In the forced vibration tests carried out by Sarpkaya [6] and Chen et al. [9], the force components have been shown to depend on Y and U_r. Since Y is mainly affected by ζ_s and M_r, and U_r is related to Re and the f_n of the cylinder, the inability of Prediction 1 to replicate the Y_{max} results of the three other experiments is consistent with their findings. Therefore, the present calculations suggest that the effects of ζ_s and M_r have to be accounted for in the determination of the force components.

An effort is made to account for the influence of ζ_s and M_r in the present model. The idea is to express the force component as a function of these parameters using available experimental data. In the present model, the experimental data of Griffin and Koopmann [7] and So et al. [24] are used and a second order polynomial fitting of the data is carried out.

The first step is to consider the influence of ζ_s by constructing a relation between the force component and ζ_s. The resulting relation is expressed as

$$C_{y1,d}^{(1)} = (-262.5844)\zeta_s^2 + (7.0481)\zeta_s + 0.0452. \tag{26}$$

In turn, this relation is used to determine the force components for the model. The model is then used to calculate the vibration amplitudes of the four cases again. The results are given in Table 4 as Prediction 2. It can be seen that a much better prediction is obtained for most of the cases considered with a ζ_s varying from a low of $0.00008 + 0.0001\,Y^2$ [27] to a high of 0.03 [24]. The revised model is able to predict fairly well the cases where ζ_s lies in the range $0.00033 < \zeta_s < 0.03$. The most important point to note is the fact that the prediction of the So et al. [24] case has not been compromised.

As for the effect of M_r, the second step is taken to express the force component as a function of the reduced damping, $\delta_r = 2\pi\zeta_s M_r$, which represents the effects of both ζ_s and M_r. The resulting relation between $C_{y1,d}^{(1)}$ and δ_r is expressed as

$$C_{y1,d}^{(1)} = (2.4906 \times 10^{-4})\delta_r^2 + (-2.1622 \times 10^{-2})\delta_r + (5.3491 \times 10^{-2}). \tag{27}$$

This relation is used to determine the force components for the model, then to calculate the vibration amplitudes of the four cases again. The results are given in Table 4 as Prediction 3. The improvement of the predictions does not seem to be very significant.

Furthermore, the present model is compared with a s.d.o.f. model developed by Sarpkaya [6]. The comparison is also given in Table 4. The set of force components used in Sarpkaya's [6] model was expressed as a function of Y and U_r. Therefore, Sarpkaya [6] has indirectly accounted for the effects of M_r and ζ_s. This is why his predictions are so close to measurements. The present model gives better predictions compared to those reported by Sarpkaya [6], but it should be noted that the force components used are partially based on the measured data of Systems I and II. These results are further evidence that accounting for the effects of M_r and ζ_s is important for the determination of the force components.

The present model is also used to calculate the variation of Y_{max} with U_r (reduced velocity) for the experimental case of Khalak and Williamson [28, 29]. In the calculation, the whole regime is divided into two sub-regimes; one is the off-resonance regime, and the other is the resonance regime. The resonance sub-regime in the experiment spanned $U_r = 5-11$. In Fig. 4 are shown the comparisons of experimental measurements and the predictions using the present model before and after modification. In the model before modification, the force components obtained from the

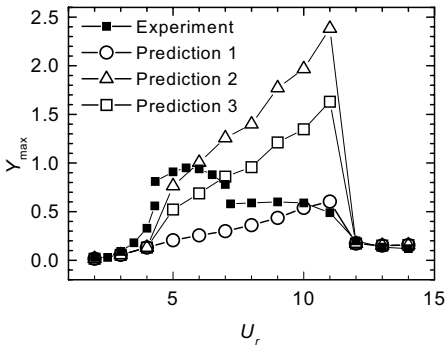

Fig. 4. Comparison of the predicted maximum vibration amplitude of an elastically mounted rigid cylinder in a cross flow with experimental measurements [28,29].

resonance and off-resonance cases based on the experiments of So et al. [24] are used to predict cylinder vibrations in these two sub-regimes, respectively, designated as Prediction 1 in the figure. The prediction of the cylinder response in the off-resonance regime agrees quite well with experimental measurements. It is seen that the model before modification can predict the sudden jump from the resonance regime to the off-resonance regime and gives a Y_{max} prediction similar to that of the 'lower' branch, but fails to predict the 'upper' branch in the resonance regime. The model after modification is used to predict the resonance case, designated as Predictions 2 and 3 in the figure. It is seen that a far more reasonable prediction is obtained, particularly, the sudden jump from the off-resonance regime to the 'upper' branch is reproduced. It would be interesting to note that Prediction 3 appears to be better than Prediction 2, implying that taking into account the influences of both M_r and ζ_s may be advantageous for a wide range of U_r, although the improvement may not be obvious at a single value, as seen in Table 4.

In spite of the improvement, the prediction of the lock-in regime is not quite satisfactory. This may be partially due to the fact that the implementation of the model is based on the interpolation of experimental data. Since the model is developed as an iteration process, an alternative way is to update the fluid force components in each step of the iteration. However, this requires an accumulation of a set of fluid force components as a function of vibration amplitude and shedding frequency in both the lift and drag directions.

5. Conclusions

A non-linear fluid force model is developed for the analysis of vortex-induced vibration of a fix-supported single cylinder in a cross flow. The vibration effects in the transverse and streamwise directions are considered in the context of a 2.d.o.f. structural model. In the proposed model, the lift and drag forces are assumed to be sinusoidal at f_s and $2f_s$ for a stationary cylinder, respectively, and the fluid–cylinder interaction introduces higher harmonics. This gives rise to a nonlinear representation of the fluid force. The model is then extended to a finite elastic cylinder using the modal analysis approach. Therefore, the effect of vibration mode is also accounted for in addition to the fluid–structure interaction effect.

First, the model is used to evaluate fluid force components from experimental data obtained from a freely vibrating cylinder in a cross flow. Formulae relating the fluid force components and the vibration displacements are derived. The required amplitude and frequency data in the formulae are calculated by carrying out a spectral analysis of the time series of structural vibration using the ARMA technique. An example is given to demonstrate the evaluation procedure. The fluid force results for a resonance case and an off-resonance case are presented. It is shown that non-linear force components are present at resonance.

The model is then used to predict vortex-induced vibration of an elastic cylinder fix-supported at both ends using the fluid force components thus deduced. This model prediction is designated as Prediction 1. Three experimental cases previously reported [7,27–29] are calculated and compared with the predictions of Sarpkaya [6], who used an s.d.o.f. model. The results of Prediction 1 partially agree with experimental measurements, and the discrepancy could be attributed to the dependence of the fluid force components on ζ_s and M_r. In order to improve the force model further, an attempt is made to account for the effects of M_r and ζ_s by constructing a relation between the fluid force components and ζ_s and M_r. Two relations are deduced, one is between the fluid force components and ζ_s, and the other is between the fluid force components and the reduced damping, δ_r, which includes the effects of both ζ_s and M_r. The modified model, designated as Predictions 2 and 3, respectively, is again used to calculate the experimental cases considered. The results are much improved. A further comparison of the model before and after modification with the Y_{max} data measured by Khalak and Williamson [28,29] for a range of U_r also reveals good agreement. Particularly, the sudden jump at the transition points between the off-resonance and the resonance regimes is reproduced. An iteration procedure is suggested, which may further improve the prediction of the present model.

Acknowledgements

Funding support from the Research Grants Council under Grant Nos. PolyU5159/97E and PolyU5128/98E is gratefully acknowledged. Also, XQW wishes to acknowledge the Research Fellowship awarded to him by The Hong Kong Polytechnic University.

Appendix A. Fluid force coefficients

Note that using Eqs. (5a), (5b), (7a) and (7b), we have $Y(t) = Y_{max} \sin \omega_s t$, then $\dot{Y}(t) = \omega_s Y_{max} \cos \omega_s t$. Substituting this expression into Eqs. (4a) and (4b), we have

$$c_x(t) = c_D(t) - c_L(t)\omega_s Y_{max} \cos \omega_s t, \tag{A.1a}$$

$$c_y(t) = c_D(t)\omega_s Y_{max} \cos \omega_s t + c_L(t). \tag{A.1b}$$

Substituting the expressions for $c_x(t)$ and $c_y(t)$, Eqs.(7a) and (7b), into Eqs. (A.1a) and (A.1b), we have

$$c_x(t) = [\bar{C}_D + C_D \sin(2\omega_s t + \phi_D)] - [C_L \sin(\omega_s t + \phi_L)]\,[\omega_s Y_{max} \cos \omega_s t], \tag{A.2a}$$

$$c_y(t) = [\bar{C}_D + C_D \sin(2\omega_s t + \phi_D)]\,[\omega_s Y_{max} \cos \omega_s t] + [C_L \sin(\omega_s t + \phi_L)]. \tag{A.2b}$$

Expanding Eqs.(A.2a) and (A.2b), respectively, and writing the results in the form of triangular series as

$$c_x(t) = C_x^{(0)} + C_{x,m}^{(2)} \sin 2\omega_s t + C_{x,d}^{(2)} \cos 2\omega_s t, \tag{A.3a}$$

$$c_y(t) = C_{y,m}^{(1)} \sin \omega_s t + C_{y,d}^{(1)} \cos \omega_s t + C_{y,m}^{(3)} \sin 3\omega_s t + C_{y,d}^{(3)} \cos 3\omega_s t. \tag{A.3b}$$

The coefficients are

$$C_x^{(0)} = \bar{C}_D - \tfrac{1}{2} C_L \omega_s Y_{max} \sin \phi_L,$$

$$C_{x,m}^{(2)} = C_D \cos \phi_D - \tfrac{1}{2} C_L \omega_s Y_{max} \cos \phi_L,$$

$$C_{x,d}^{(2)} = C_D \sin \phi_D - \tfrac{1}{2} C_L \omega_s Y_{max} \sin \phi_L,$$

$$C_{y,m}^{(1)} = C_L \cos \phi_L + \tfrac{1}{2} C_D \omega_s \, Y_{max} \cos \phi_D$$

$$C_{y,d}^{(1)} = \bar{C}_D \omega_s Y_{max} + C_L \sin \phi_L + \tfrac{1}{2} C_D \omega_s Y_{max} \sin \phi_D,$$

$$C_{y,m}^{(3)} = \tfrac{1}{2} C_D \omega_s \, Y_{max} \cos \phi_D,$$

$$C_{y,d}^{(3)} = \tfrac{1}{2} C_D \omega_s Y_{max} \sin \phi_D,$$

Appendix B. Nomenclature

c	damping coefficient of the cylinder
c_L, c_D	lift and drag force coefficients
c_x, c_y	fluid force coefficients in the streamwise and the transverse directions
$\bar{C}_D$	mean drag coefficient
C_{L0}, C_{D0}	lift and drag coefficients
$C_{x,m}^{(\bullet)}$, $C_{x,d}^{(\bullet)}$,	fluid force components along the x direction with subscript m denoting fluid inertia, d denoting fluid damping, and the dot represents the order of the harmonics
$C_{y,m}^{(\bullet)}$, $C_{y,d}^{(\bullet)}$	fluid force components along the y direction with m, d and the dot having the same meaning as above
EI	bending stiffness of the cylinder
f_L, f_D	dimensionless lift and drag force, respectively
f_y, f_x	dimensionless force component along the y and x directions, respectively
f_s	vortex shedding frequency
f_{ni}^*	dimensional natural frequency
f_{xn}, f_{yn}	nth modal dimensionless fluid force in the x and y direction
F_L, F_D	dimensional lift and drag force, respectively
F_y, F_x	dimensional force component along the y and x directions, respectively
m	mass per unit length of the cylinder
M_r	mass ratio
Re	Reynolds number based on cylinder diameter and free stream velocity

U_∞	free stream velocity
$U_{ri} = U_\infty D/f_{ni}^*$	reduced velocity, i represents the ith natural frequency
$W_n(z)$	the expression of mode shape of the nth normal mode
$\bar{X}$	static displacement of the cylinder
X, Y	cylinder displacements in the streamwise and the transverse directions
$\dot{X}$, $\dot{Y}$	cylinder velocities in the streamwise and the transverse directions
X_n, Y_n	nth modal displacements of an elastic cylinder in the streamwise and the transverse directions
Greek letters	
θ	the angle between the direction of the uniform flow and the instantaneous velocity vector of the cylinder vibration
$\omega_s = 2\pi f_s$	angular frequency of vortex shedding
$\omega_{n0} = 2\pi f_{n0}$	angular natural frequency of a stationary cylinder
ϕ_L, ϕ_D, ϕ_X	phase angles
ζ_s	structural damping ratio
ζ_{sn}	structural damping ratio of the nth normal mode
δ_r	reduced damping

References

[1] R.D. Blevins, Flow-Induced Vibration, 2nd Edition, Krieger, New York, 1994.
[2] W.K. Blake, Mechanics of Flow-Induced Sound and Vibration, Academic, New York, 1986.
[3] G. Parkinson, Phenomena and modeling of flow-induced vibrations of bluff bodies, Progress in Aerospace Science 26 (1989) 169–224.
[4] T. Sarpkaya, Vortex-induced oscillations—a selective review, Transactions of the American Society of Mechanical Engineers, Journal of Applied Mechanics 46 (1979) 241–258.
[5] P.W. Bearman, Vortex shedding from oscillating bluff bodies, Annual Review of Fluid Mechanics 16 (1984) 195–222.
[6] T. Sarpkaya, Fluid forces on oscillating cylinders, American Society of Civil Engineers, Journal of the Waterway, Port, Coastal and Ocean Division WW4 (1978) 275–291.
[7] O.M. Griffin, G.H. Koopmann, The vortex-excited lift and reaction forces on resonantly vibrating cylinders, Journal of Sound and Vibration 54 (1977) 435–448.
[8] O.M. Griffin, Vortex-excited cross-flow vibrations of a single cylindrical tube, Transactions of the American Society of Mechanical Engineers, Journal of Pressure Vessel Technology 102 (1980) 158–166.
[9] S.S. Chen, S. Zhu, Y. Cai, An unsteady flow theory for vortex-induced vibration, Journal of Sound and Vibration 184 (1995) 73–92.
[10] R.T. Hartlen, I.G. Currie, Lift oscillation model for vortex-induced vibration, American Society of Civil Engineers, Journal of Engineering Mechanics 96 (1970) 577–591.
[11] R.E.D. Bishop, A.Y. Hassan, The lift and drag forces on a circular cylinder in a flowing fluid, Proceedings of the Royal Society A277 (1964) 32–50.
[12] W.D. Iwan, R.D. Blevins, A model for vortex induced oscillation of structures, Transactions of the American Society of Mechanical Engineers, Journal of Applied Mechanics 41 (1974) 581–586.
[13] R.A. Skop, O.M. Griffin, A model for the vortex-excited resonant response of bluff cylinders, Journal of Sound and Vibration 27 (1973) 225–233.
[14] O.M. Griffin, R.A. Skop, G.H. Koopmann, The vortex-excited resonant vibrations of circular cylinders, Journal of Sound and Vibration 31 (1973) 235–249.

[15] R. Landl, A mathematical model for vortex-excited vibrations of bluff bodies, Journal of Sound and Vibration 42 (1975) 219–234.
[16] E. Berger, On a mechanism of vortex excited oscillations of a cylinder, Journal of Wind Engineering and Industrial Aerodynamics 28 (1988) 301–310.
[17] S. Balasubramanian, R.A. Skop, A nonlinear oscillator model for vortex shedding from cylinders and cones in uniform and shear flows, Journal of Fluids and Structures 10 (1996) 197–214.
[18] R.A. Skop, O.M. Griffin, On a theory for the vortex-excited oscillations of flexible cylindrical structures, Journal of Sound and Vibration 41 (1975) 263–274.
[19] W.D. Iwan, The vortex induced oscillation of elastic structural elements, Transactions of the American Society of Mechanical Engineers, Journal of Applied Mechanics 42 (1975) 1378–1382.
[20] R.D. Blevins, T.E. Burton, Fluid forces induced by vortex shedding, American Society of Mechanical Engineers Journal of Fluids Engineering 98 (1976) 19–26.
[21] D.E. Capone, G.C. Lauchle, Modeling the unsteady lift and drag on a finite-length circular cylinder in cross-flow, Transactions of the American Society of Mechanical Engineers, Journal of Fluids and Structures 14 (2000) 799–817.
[22] M.P. Mignolet, J.R. Red-Horse, ARMAX identification of vibrating structures: model and model order estimation, Proceedings of the 35th Structures, Structural Dynamics, and Materials Conference, AIAA/ASME/ASCE/AHS/ASC, Hilton Head, SC, 1994, pp. 1628–1637.
[23] J. Olinger, K.R. Sreenivasan, Nonlinear dynamics of the wake of an oscillating cylinder, Physical Review Letters 60 (1988) 797–800.
[24] R.M.C. So, Y. Zhou, M.H. Liu, Free vibrations of an elastic cylinder in a cross flow and their effects on the near wake, Experiments in Fluids 29 (2000) 130–144.
[25] Y. Zhou, R.M.C. So, Z.J. Wang, Free vibrations of two fix-supported elastic cylinders, in: S. Ziada, T. Staubli (Eds.), Flow Induced Vibration, Proceedings of the 7th International Conference on Flow-Induced Vibration, FIV 2000, Lucerne, Switzerland, A.A. Balkema, Rotterdam, 2000, pp. 45–52.
[26] S. Granger, A new signal processing method for investigating fluidelastic phenomena, Journal of Fluids and Structures 4 (1990) 73–97.
[27] D. Brika, A. Laneville, Vortex-induced vibrations of a long flexible circular cylinder, Journal of Fluid Mechanics 250 (1984) 481–508.
[28] A. Khalak, C.H.K. Williamson, Dynamics of a hydroelastic cylinder with very low mass and damping, Journal of Fluids and Structures 10 (1996) 455–472.
[29] A. Khalak, C.H.K. Williamson, Fluid forces and dynamics of a hydroelastic structure with very low mass and damping, Journal of Fluids and Structures 11 (1997) 973–982.